STRUCTURAL PERFORMANCE EVALUATION OF WOODEN FRAME WITH CFRTP REINFORCEMENT

Hina Takizawa*,Hiroki Matsumoto,Nobuji Sakurai ***,Kiyoshi Uzawa**,Yuya Takaiwa***
Dept. of Architecture, Faculty of Science and Engineering, Toyo University,
**** ICC, Kanazawa Institute of Technology ,***
*****Nose Structural Corporation Co., Ltd***

Keywords: *Carbon Fiber, Thermoplastic, Shear Wall, Construction Field*

Abstract

In this study, in-plane shear tests of a wooden frame wall reinforced with CFRTP strands were performed to clarify the structural performance. The developed CFRTP sockets with toughness were applied to the end fixing structure of the CFRTP strand, and they were confirmed that deformation (1/10 rad). This is a useful result from the viewpoint of adaptation to seismic retrofitting of cultural property buildings, which require deformation performance of about 1/30 rad, and in some cases about 1/15 rad, for extremely rare earthquakes.

1 General Introduction

Carbon fiber reinforced plastics have the characteristics of high strength, light weight, resistance to rust, and no condensation, and are attracting attention in the architectural field [1], [2] as well. The material often used for seismic retrofitting today is building steel. It has a long history, and since it was adapted to the reinforcement of the *Todaiji* Temple *Kondo* in the Meiji era, it has been adapted to many wooden buildings of cultural properties. However, seismic retrofitting using building steel may adversely affect the wooden members of wooden buildings due to dew condensation. In view of such circumstances, there is an example [3] in which a strand (CFRTP strand) made of a carbon fiber reinforced thermoplastic is applied to a seismic retrofitting member of wooden buildings. Here, since carbon fiber reinforced plastics do not have toughness like building steel materials, they cannot be applied to vertical structural surfaces that must tolerate large deformation during an earthquake and adapted to horizontal structures that do not cause large deformation Therefore, in the context of the above background, the authors have developed and proposed the edge of CFRTP strand using a CFRTP socket using a heat welding method in order to resolve the problem of brittle fracture without impairing the features of CFRP [4]. In the process of its development, it was confirmed that when the grain direction of socket and the grain direction of strand are aligned, the socket has relatively high strength but brittle fracture, and if not aligned, the socket is low but brittle fracture does not occur [5]. It has also been confirmed that the strength is improved by increasing the heating temperature and volume [6]. In this report, we perform a static in-plane shear test of a wooden seismic retrofit wall to which the end fixing structure of the tough CFRTP strand proposed in [5] and [6] has been applied. By understanding the strength and fracture form, we will examine the applicability of vertical structural surfaces of wooden buildings to seismic retrofitting.

2 The Outline of Specimen

2.1 Details of Specimen

Assuming the vertical plane of a wooden house, a static in-plane shear tests were conducted using a specimen with a wall length of 910 mm, which is a module of a general wooden building. Three specimens each with height of 2910 mm and width of 910 mm were carried out. Table.1 shows the specifications of the specimens, Table.2 shows each member of the specimens, and Fig.1 shows the specimen diagram. When the specimens were manufactured, the frequency was measured using the longitudinal vibration method [7], and the bending Young's modulus of the member was obtained as a reference value from the predominant natural frequency obtained by the measurement. The results of measuring the moisture content of the members at

that time with a capacitive moisture meter are also shown. For the dimensions in the table1, the cross-sectional dimensions were measured with a caliper and the length dimensions were measured with a tape measure. The density in Table2 is the value obtained by dividing the weight measured by the weight scale by the volume.

Table 1. Specifications of Specimen

No.	Cross section (mm)	The number of specimen	The torque value (Nm)	Corbels of CFRTP
910-1	910×2910	1	10	nothing
910-2			2	nothing
910-3				screwed

Table 2. Each Member of Specimen

No.	Elements	Moisture content (%)	Bending Young modulus (kN/mm^2)	Density (kg/m^3)
910-1	Column A	29.6	7.4	641.8
	Column B	25	5.5	661.3
	Beam	20.9	10.5	502.1
	Foundation	15.5	11.6	632.8
910-2	Column A	31.7	9.2	557.0
	Column B	31	7.9	631.7
	Beam	13.6	11.1	453.8
	Foundation	29.2	10.3	563.5
910-3	Column A	28.4	5.7	628.1
	Column B	23.9	8.9	508.0
	Beam	13	11.5	472.2
	Foundation	25.3	11.8	551.8

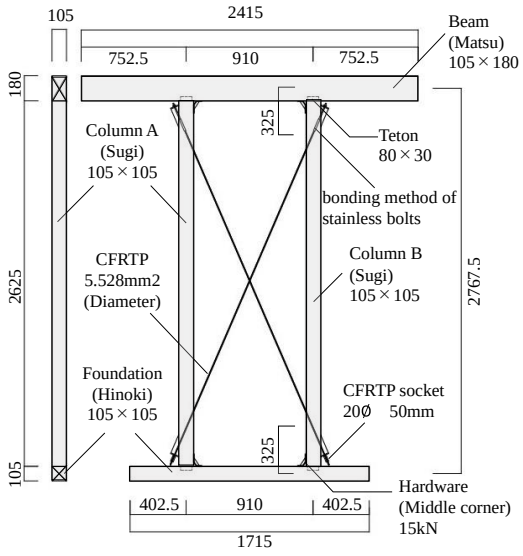

Fig. 1 Specimen Diagram

2.2 CFRTP Socket Element Test

The tensile modulus of the CFRTP strand used is 110 kN/mm^2. The CFRTP strand is composed 7 twisted wires with a diameter of 2.1mm, and the cross-sectional area is 24 mm^2. The structure of edge of the CFRTP strands consists of two types. One side is the CFRTP socket, which has been shown to be ductile fracture at about 15 kN from experiments. The other side is bonding method of stainless bolts, the guaranteed load is larger than the breaking load of the CFRTP socket, causing brittle fracture. Since the CFRTP socket yields in advance, the CFRTP strand has toughness. Fig.2 shows the results of tensile test of the CFRTP socket of the rod of the same specifications that is suitable for the test. The test method was based on previous studies [6]. As a result of the test, it was confirmed that the behavior of the CFRTP sockets were that there was no brittle fracture even if the first yield point due to adhesive yielding, the second yielding point when the maximum yield strength was reached, and then a displacement of 40 mm occurred. Specimen 910-1 had a torque value of 10 Nm for stainless bolts of the end of the CFRTP strand. The corbel that receives the end of the CFRTP strand was not fixed with screws, allowing slippage. The torque value of Specimen 910-2 is 2 Nm (about hand tightening), and the screw of the corbel is not fixed. The torque value of Specimen 910-3 was 2 Nm, and the corbel was fixed with screws at four locations. Fig.3 shows how to fix the corbel.

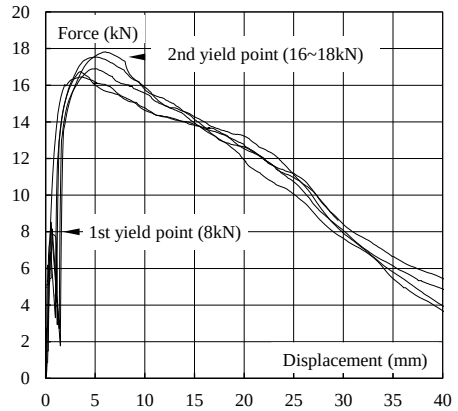

Fig. 2 CFRTP socket Force-Displacement Relationship

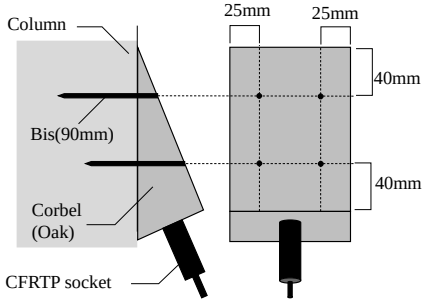

Fig. 3 How to Fix the Corbel with Bis

2.3 Preliminary Analysis by FEM

Preliminary analysis of the wooden frame reinforced with CFRTP strands was performed by finite element analysis. Modeling was performed by linearly transforming the members of the specimen. The support condition constrains the movement of the model in the XZ plane in the X and Z directions, not the rotation. The joining condition of the members was pin joining by releasing the flexural rigidity of both ends in the y and z directions of the element coordinate system.

The short-term allowable stress of column is 14.8N/mm^2, when it is assumed that minimum cross-sectional dimension of the structural pillar used in a general house is 105 mm × 105 mm, and the non-grade material with the lowest strength among the tree species of the pillar used is too much. By analysis, it was confirmed that the maximum bending stress of the column was 8.8 kN, which was less than the short-term allowable stress. It was confirmed that the maximum shear force of the wooden frame reinforced with CFRTP strands was 5.2 kN, and the shear deformation angle reaching the second yield point of the socket was 1/45 rad.

3 In-Plane Shear Test

3.1 Method and measurement plan of in-plane shear test

An oil jack is used to horizontally apply a positive and negative load to the specimen. The loading device is fixed column base. The specimen is fixed with an in-plane jig, and the foundation is fixed to the beam to fix to the specimen. In the loading cycle (repetition history), the apparent shear deformation angle of the specimen is ± 1/450, ± 1/300, ± 1/200, ± 1/150, ± 1/100, ± 1/75, ± 1/50 rad. Deformation control is performed three times, and a positive and negative load is performed once with a deformation angle of ± 1/30 rad. After that, the specimen is loaded until the maximum load is reached and the load drops (0.8Pmax) or a deformation angle reaches 1/10 rad or more. Fig.4 shows repetition history. Horizontal displacement of the top of the specimen, horizontal displacement of the base of the specimen, horizontal displacement of the column, vertical displacement of the column (2 points), vertical displacement of the fixed beam (2 points), horizontal displacement of the fixed beam, and vertical displacement of the jig (2 points) are measured. The measurement points used for analysis are shown in Fig.5 and Fig.6, and Fig6 shows back side of experiment device and specimen. In addition, the strain is measured with a strain gauge at 8 points, 2 points each on the front and back of the CFRTP strands and 4 points on the wooden part.

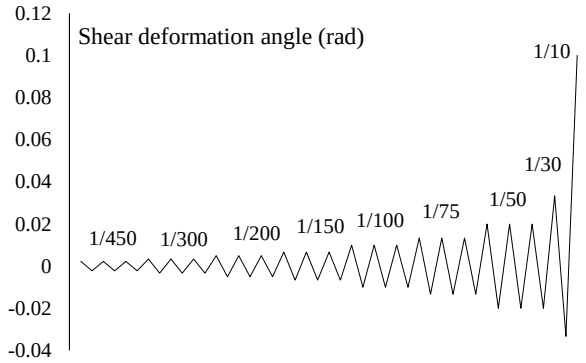

Fig. 4 Repetition History

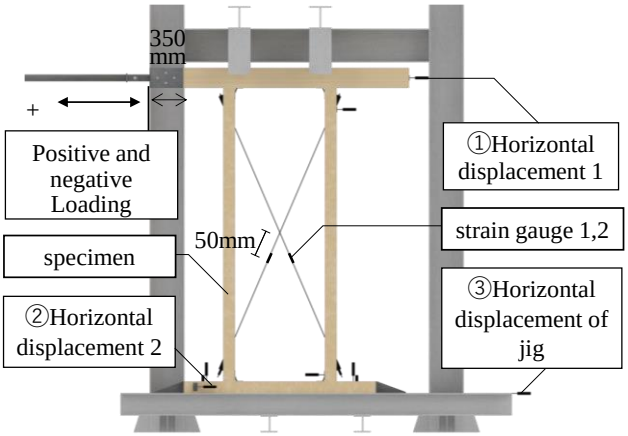

Fig. 5 The Experimental Device and Specimen

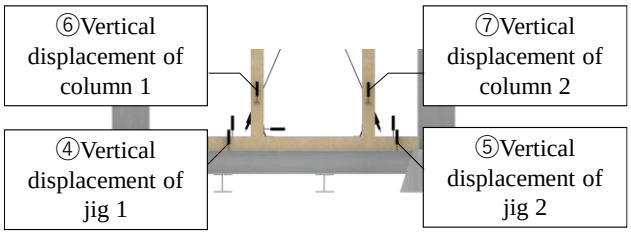

Fig. 6 Points of Measurement on the Back of Specimen

3.2 Shear Force-Shear Deformation Angle Relationship

The relationship between the load of each specimen and the apparent shear deformation angle is shown in Fig. 7 to Fig. 10, respectively. Specimen 910-1 with a CFRTP strand stainless bolt torque value of 10 Nm had a lower maximum yield strength than Specimen 910-2 with a torque value of 2 Nm. It is

presumed that this is due to the fact that the initial tension force deformed the framework inside the premises and the CFRTP strands slackened, reducing the rigidity of the specimen. Therefore, Specimen 910-3 tightened the torque at 2 Nm. In addition, by sliding the corbel receiving the end of the CFRTP strand without fixing it, large deformation is allowed. It was confirmed that the test Specimens 910-1 and 910-2 with the specifications did not reach the first yield point up to a shear deformation angle of 1/10 rad. After the test, CFRTP strands were sunk into Columns. Specimen 910-3 with the corbel fixed reached the first yield point at 1/25 rad, and strands came off from the socket at 1/10 rad. The maximum yield stress was the highest among the three test specimens, which was 6.39 kN. Compared with the result of the preliminary analysis in Chapter 2, it is 5.2kN. In the preliminary analysis, the joint of the framework was used as a pin, and since this effect was not taken into consideration, a difference of about 1 kN occurred, but it was confirmed that the expected potential was exhibited.

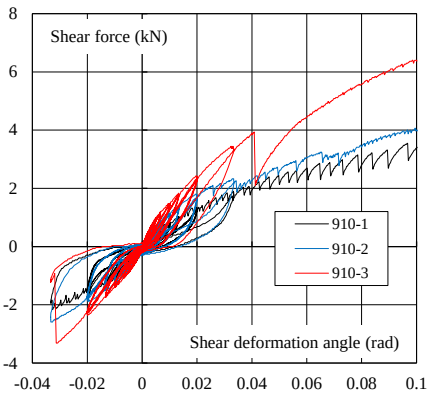

Fig. 7 Shear Force-Shear Deformation Angle Relationship (910-1,2,3)

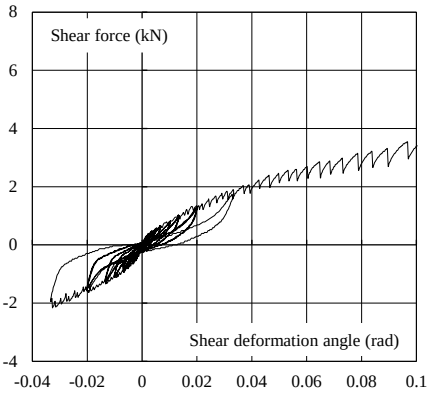

Fig. 8 Shear Force-Shear Deformation Angle Relationship (910-1)

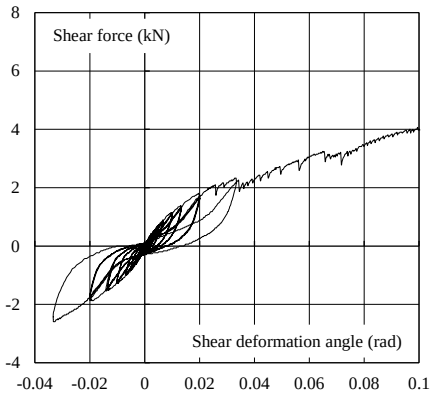

Fig. 9 Shear Force-Shear Deformation Angle Relationship (910-2)

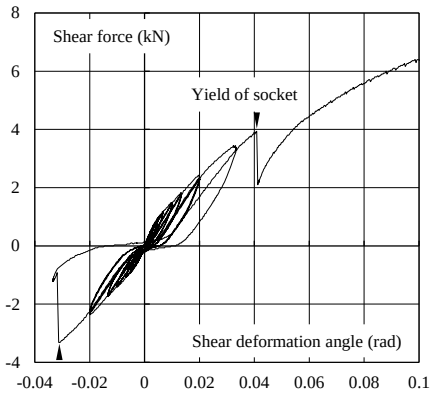

Fig. 10 Shear Force-Shear Deformation Angle Relationship (910-3)

3.3 Strain of CFRTP Strand-Shear Deformation Angle Relationship

Discuss the axial force that the CFRTP strand bears. Here, we focus on the Specimen 910-3, which is presumed to have reached the first yield point of the socket. The strain-shear deformation angle relationship of the CFRTP strands obtained from the strain gauge 1 and strain gauge 2 attached to the CFRTP strand is shown in Fig. 11 and Fig. 12, respectively. Both data showed similar values, with a maximum strain of 0.00531. The elastic modulus and cross-sectional area of the CFRTP strand are known values, and the axial force generated in the CFRTP strand was calculated assuming that the tensile elastic modulus was 110 GPa and the cross-sectional area was 24 mm^{2}. Fig.13 and Fig.14 show the relationship between strain and shear deformation angle, respectively. It was confirmed that the Specimen 910-3 bears a maximum axial force of 14 kN. In addition, the load applied to the CFRTP strand at the shear deformation angle, which is estimated to have reached the first yield point of the CFRTP socket, is

7.8 kN, which is consistent with the result of the element test described in Chapter 2. After the CFRTP socket yielded, it was confirmed that the socket was gradually pulled out and had toughness.

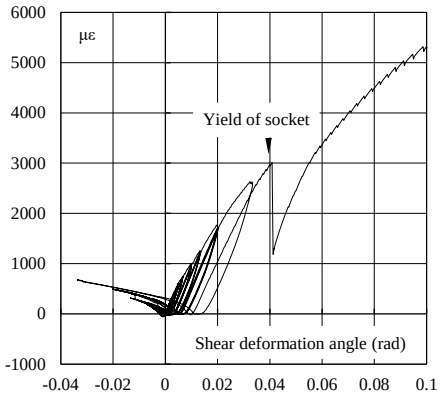

Fig. 11 Strain of CFRTP Strand-Shear Deformation Angle Relationship (Strain gauge-1) (910-3)

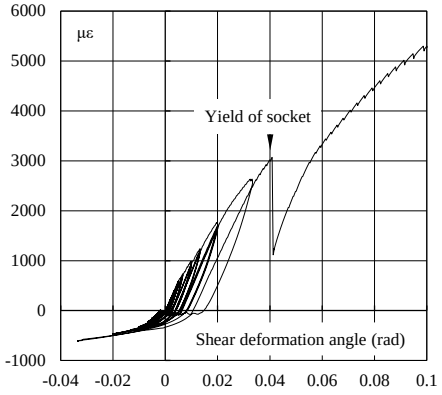

Fig. 12 Strain of CFRTP Strand-Shear Deformation Angle Relationship (Strain gauge-2) (910-3)

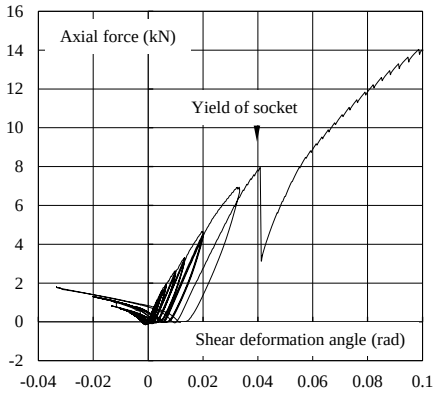

Fig. 13 Axial Force of CFRTP Strand-Shear Deformation Angle Relationship (Strain gauge-1) (910-3)

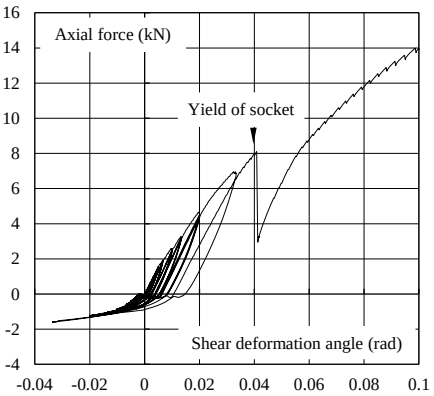

Fig. 14 Axial Force of CFRTP Strand-Shear Deformation Angle Relationship (Strain gauge-2) (910-3)

4 Analysis of Shear Deformation Mechanism of Specimen

4.1 Indentation Deformation of CFRTP Strand

Analyze the factors that contributed to the shear displacement of the specimen. The analysis assumes the mechanism shown in Fig. 15 and evaluates the contribution rate of each mechanism to shear displacement.

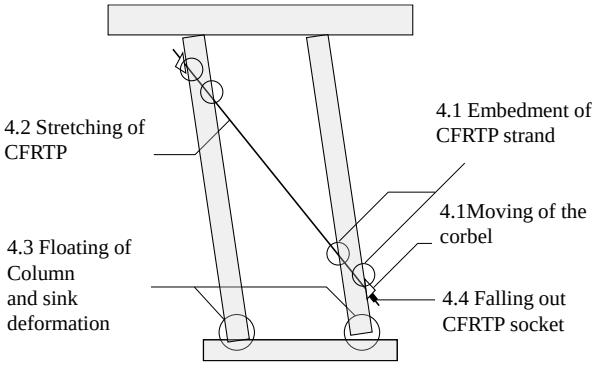

Fig. 15 Factors Contributed to the Shear Deformation

First, we analyze the behavior of CFRTP strands and columns due to embedment. When the CFRTP strand is sunk into the column, the planar geometric position of the CFRTP strand changes and the length becomes shorter than the original length, causing displacement of top of column for the excess length. This is the same phenomenon as the CFRTP strand is stretched. Since the amount subtracted from the length of the original strand is the amount of displacement that contributes to the displacement of the top of the column, the displacement is calculated from the geometrical relationship. Fig.16 to Fig.18,

the calculation formula shows the situation when the CFRTP strand is sunk.

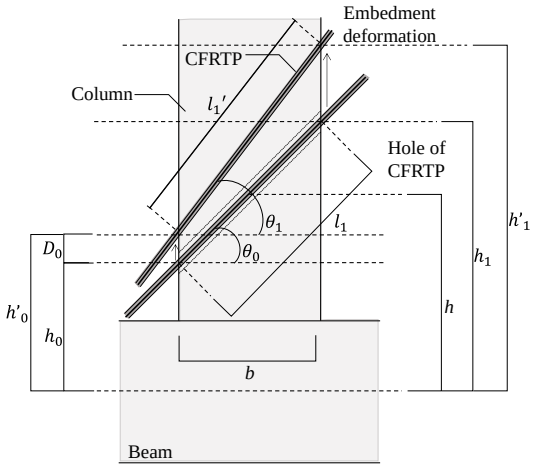

Fig. 16 Change in Length CFRTP Strand

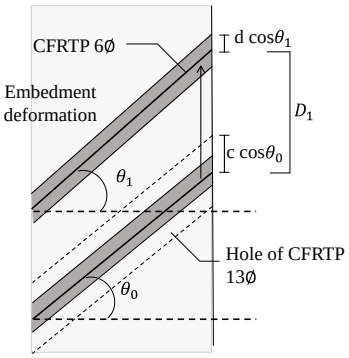

Fig. 17 Detail of Embedment Deformation

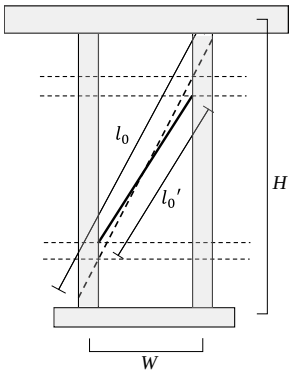

Fig. 18 Embedment Deformation

$$tan\theta_0 = \frac{(H-2h)}{W} \quad (1)$$

$$h_0 = h - \frac{b}{2}tan\theta_0 \quad (2)$$

$$h_1 = h + \frac{b}{2}tan\theta_0 \quad (3)$$

$$h_0' = h_0 + D_0 + \mathrm{c}\ con\theta_0 - \mathrm{d}\ \cos\theta_1 \quad (4)$$

$$h_1' = h_1 + D_1 + \mathrm{c}\ con\theta_0 - \mathrm{d}\ \cos\theta_1 \quad (5)$$

$$l_1' = \sqrt{(h_1' - h_0')^2 + b^2} \quad (6)$$

Here,

h : The position of CFRTP strand at centroid of column (325mm)

h_0: The position of CFRTP strand at inside of specimen (447mm)

h_1:The position of CFRTP strand at outside of specimen (202mm)

θ_0: Angle of the CFRTP strand

θ_1: Angle of the CFRTP strand after deformation

D_0: embedment deformation outside of specimen

D_1: embedment deformation inside of specimen

h_0': The position of CFRTP strand at inside of specimen after embedment deformation

h_1': The position of CFRTP strand at outside of specimen after embedment deformation

l_1': The length of CFRTP strand internal the column

W: Specimen width (910mm)

H: Specimen length (2767.5mm)

b: Column width (105mm)

c: Radius of hole for CFRTP strand (6.5mm)

d: Radius of CFRTP rod(3mm)

Here, since the end fixing of the CFRTP strand uses two types of specifications, the amount of penetration differs between the two columns, so the length of the CFRTP strand when it is embedded in both columns is calculated.

$$l_0' = \sqrt{(H - h_1' - h_0')^2 + (W-b)^2} \quad (7)$$

$$\Delta l_{4.1} = (l_0 + 2l_1) - (l_0' + l_1' + l_2') \quad (8)$$

Here,

$\Delta l_{4.1}$: elongation of the CFRTP strand due to embedment of CFRTP strand before embedment deformation

l_0: The length of CFRTP strand inside specimen

l_0': The length of CFRTP strand inside specimen after embedment deformation

l_1: The length of CFRTP strand internal the column before embedment deformation

l_2': The length of CFRTP strand internal the other side column after embedment deformation

Fig.19 shows the figure when calculating displacement of top of the column because the CFRTP strand has stretched.

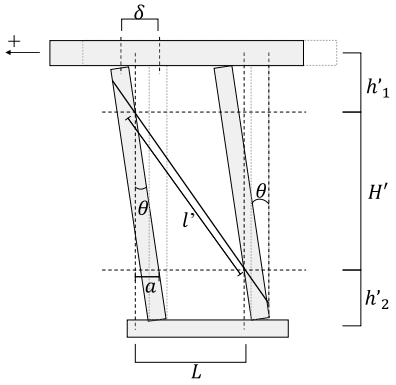

Fig. 19 Calculating Displacement

$$l' = l_0 + \Delta l \tag{9}$$

$$l' = \sqrt{h_1'^2 + (W - b + a)^2} \tag{10}$$

$$a = \sqrt{h_1'^2 - l'^2} - (\mathrm{W} - \mathrm{b}) \tag{11}$$

$$\delta_{4.1} = \frac{a}{H'}\mathrm{H} = \frac{\sqrt{h_1'^2 - l'^2} - (\mathrm{W} - \mathrm{b})}{H'}\mathrm{H} \tag{12}$$

Here,
l': The length of CFRTP strand inside specimen after embedment deformation
a: Horizontal deformation at the position of mounting CFRTP strand inside specimen
H': The length of CFRTP strand inside specimen after embedment deformation
$\delta_{4.1}$: The deformation of the top of the column due to embedment of CFRTP strand

4.2 Axis Deformation of CFRTP Strand

The formula for calculating the elongation when a tensile force acts on the CFRTP strand and deformation is shown. The tensile modulus of the CFRTP strand shall be 110 GPa and the cross-sectional area shall be 24 mm^2. The elongation was calculated from the average value of the strains of the strain gauge 1 and the strain gauge 2 of the CFRTP strand obtained by the experiment. The CFRTP strand is calculated assuming that it extends uniformly in the length direction and in the cross section.

$$\sigma = E\varepsilon \tag{13}$$

$$\Delta l_{4.2} = \frac{Pl}{AE} \tag{14}$$

$$l'_{4.2} = l_0 - 2l_1' + \Delta l_{4.2} \tag{15}$$

$$\delta_{4.2} = \frac{\sqrt{h_1'^2 - {l_{4.2}}'^2} - (\mathrm{W} - \mathrm{b})}{H'}\mathrm{H} - \delta_{4.1} \tag{16}$$

Here,
$\Delta l_{4.2}$: elongation of the CFRTP strand due to Load on CFRTP strand
P: Load on CFRTP strand
A: cross-sectional area of CFRTP strand (24mm^2)
E: The tensile modulus od CFRTP strand (110Gpa)
l:The whole length of CFRTP strand
$l'_{4.2}$:The length of CFRTP strand inside specimen after the deformation of elongation of the CFRTP strand due to Load
$\delta_{4.2}$: The deformation of the top of the column due to elongation of the CFRTP strand due to Load on CFRTP strand

4.3 Rotational Deformation of the Timber

Fig.20 shows a diagram for calculating the displacement of top of the column due to the lifting and sinking of columns. The number of the displacement meter used is shown in the figure.

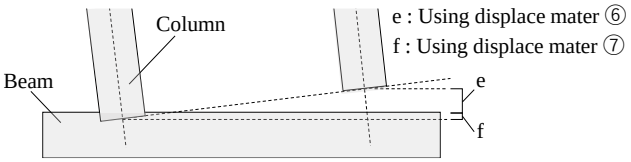

Fig. 20 Lifting and Embedment of Columns

$$\delta_{4.3} = \frac{(e + f)H}{W} \tag{17}$$

Here,
e: The length of lifting column
f: Embedment deformation of column
$\delta_{4.3}$: The deformation of the top of the column due to Lifting and sinking of columns

4.4 Fall out CFRTP socket

When the CFRTP socket is fallen out, that amount becomes the elongation of the CFRTP strand. The displacement of top of the column is calculated from the elongation of the CFRTP strand using equations (15) and (16) by replacing $\Delta l_{4.2}$ with it and replacing $\delta_{4.2}$ with the deformation of the top of the column due to falling out CFRTP socket.

4.5 Result of Analysis

Table.4 shows an estimate of the ratio of the effects of each factor that causes the shear

displacement of the specimen,4.1 is Indentation deformation of CFRTP Strand,4.2 is axis deformation of CFRTP strand,4.3 is rotational deformation of the timber,4.4 is deformation of falling out CFRTP socket. In Specimen 910-1 and Specimen 910-2, the displacement of the column is greatly affected by the lifting and sinking of the column, and in Specimen 910-3, the effect is small due to the socket being fallen out. Table3 shows each factor the causes the shear displacement.

Table 3. Each Factor Causes the Shear Displacement

	The Shear Displacement mm (%)		
	910-1	910-2	910-3
4.1	157(56.8)	152(55.1)	31.6(11.4)
4.2	20(7.4)	27(9.7)	50(18.0)
4.3	51(18.6)	48(17.5)	65.8(23.7)
4.4	0(0)	0(0)	85(30.9)
Total	229(82.8)	228(82.4)	233(84.2)

*Actual total deformation is 277mm and the value in ( ) is the ratio of shear displacement of each factor to actual total deformation.

5 Conclusion

In this study, in-plane shear tests of a wooden frame wall reinforced with CFRTP strands were performed to clarify the structural performance. The developed CFRTP sockets [6] with toughness were applied to the end fixing structure of the CFRTP strand, and they were confirmed that brittle fracture did not occur even during large deformation (1/10 rad). This is a useful result from the viewpoint of adaptation to seismic retrofitting of cultural property buildings, which require deformation performance of about 1/30 rad, and in some cases about 1/15 rad(for example [8], [9]) for extremely rare earthquakes. Analysis of the deformation mechanism of each specimen using the results obtained by the in-plane shear tests revealed that the structural performance differs depending on how the end of CFRTP strand is received in the framework. It should be noted that in Specimen 910-3 with the corbel fixed, the first yield occurred at about 1/25 rad of the socket, but it contributed to the toughness performance of the wall without brittle fracture. In the Specimen 910-1 and 910-2, the stress remained below the first yield point of the socket. It is presumed that this is because the surface of column where the corbel slipped on. In the future, when the brace angle is close to 45 degrees, it will be necessary to consider whether or not the corbel is fixed according to the situation to be used. By doing so, it is possible to deal with various structural dimensions. We would like to build knowledge that contributes to the expansion of the applicabFIGle range by examining it in the future.

Acknowledgements

This work was supported by JST COI Grant Number JPMJCE1315.

References

[1] Kiyoshi Uzawa, Yoshihiro Saito, Atsushi Hokura：APPLICATION OF COMPOSITE MATERIALS TO CIVIL ENGINEERING AND CONSTRUCTION FIELDS -NEW INITIATIVES THROUGH ADVANCED MATERIALS AND INNOVATIVE MANUFACTURING TECHNOLOGY-, Journal of Japan Society of Civil Engineers, Ser. A1 (Structural Engineering & Earthquake Engineering (SE/EE)) 73(5), II_1-II_9, 2017.5 (in Japanese)

[2] JIS A 5571:2019：Tension member for seismic reinforcement-- Carbon fibre composite strand wires, 2019.11

[3] Shoichi Ikebata, Kyoshi Uzawa: Innovative New Construction Material, Science and Tecnology Soxiety,JST Research Results, 2021

[4] Yuya Takaiwa, Katsuhiko Nunotani, Kiyoshi Uzawa : Development of tough CFRP strand end fixation , AIJ Journal of Technology and Design 27(65), pp.108-113, 2021.2

[5] Yuya Takaiwa, Katsuhiko Nunotani, Atsushi Hokura, Shiro Noguchi, Nobuaki Inui, Tadashi Sakuma, Kiyoshi Uzawa : INFLUENCE OF WELDING TEMPERATURE ON ADHESION PERFORMANCE OF CFRTP STRAND ROD-SOCKET , 16th Japan International SAMPE Symposium & Exhibition, 3A-06 , 2019.9

[6] Takaiwa Y, Hokura A and Uzawa K: Proposal of CFRTP Rod-End Fixing Using Thermal Welding Method and Bond Characteristic Evaluation, Summaries of technical papers of Annual Meeting Architectural Institute of Japan, pp.847-848, 2019

[7] Iwai S :Nondestructive of the Elastic Modulus and Investigation of Strength of Old Timber from a Wooden Old House., pp.15-18, 2006

[8] Agency for Cultural Affairs: Guidelines for Assessing Seismic Resistance of Important Cultural Properties (Buildings) , Revised on 2012. 6

[9] Agency for Cultural Affairs: Implementation Guidance for Basic Seismic Assessment of Important Cultural Properties (Buildings), Revised on 2012. 6